G02/1*

Assessment of Ductile Fracture Methodology Based on Applications to Large-Scale Experiments

B. R. BASS, C. E. PUGH, J. KEENEY-WALKER
Oak Ridge National Laboratory, Oak Ridge, TN USA
H. SCHULZ, J. SIEVERS
Gesellschaft fur Reaktorsicherheit, Koln, FRG

ABSTRACT

A summary of the present status of the Project for Fracture Analysis of Large-Scale International Reference Experiment (FALSIRE) is given. Fracture assessments compiled from Project FALSIRE for five pressurized-thermal-shock experiments are compared. Some observations are made concerning predictive capabilities of the fracture methodologies used in these assessments.

1 INTRODUCTION

Project FALSIRE was sponsored by the Fracture Assessment Group (FAG) of Principal Working Group No. 3 (CSNI - PWG/3) of the OECD/NEA's Committee on the Safety of Nuclear Installations (CSNI). On behalf of the CSNI/FAG, the USNRC's Heavy-Section Steel Technology (HSST) Program at the Oak Ridge National Laboratory and the Gesellschaft für Reaktorsicherheit (GRS), Köln, FRG had responsibility for organization arrangements related to Project FALSIRE. Motivation for the project was derived from recognition by the CSNI-PWG/3 that inconsistencies were being revealed in predictive capabilities of variety of fracture assessment methods, especially in ductile fracture applications. As a consequence, the CSNI/FAG was formed to evaluate fracture prediction capabilities currently used in safety assessments of nuclear components. Members were from laboratories and research organizations in Western Europe, Japan, and the U.S.A.

To meet its objectives, the CSNI/FAG planned an international project to assess various fracture methodologies through interpretive analyses of selected large-scale fracture experiments. A number of large-scale fracture tests have been performed in recent years in several countries, and an even larger number of organizations have become cognizant of them and employed test results in attempts to verify analytical methods. From this group, the reference experiments that were eventually selected by the CSNI/FAG for detailed analysis and interpretation are given in Table 1.

The CSNI/FAG established a common format for comprehensive statements of these experiments, including supporting information and available analysis results. These statements formed the basis for evaluations that were performed by an international group of analysts using a variety of techniques. Organizations that participated in Project FALSIRE are given in Table 2. A three-day workshop was held in Boston, Mass. during May 1990, where all participating analysts examined these evaluations in detail. A portion of the tentative results and conclusions derived from the workshop are given in the following sections.

*Research sponsored by the Office of Nuclear Regulatory Research, U.S. Nuclear Regulatory Commission under Interagency Agreement 1886-8011-9B with the U.S. Department of Energy under Contract DE-AC05-84OR21400 with Martin Marietta Energy Systems, Inc.

Table 1. Large-scale fracture experiments analyzed in CSNI/FAG Project FALSIRE.

Experiment	Testing Organization	Country
NKS-3	Materialprüfungsanstalt (MPA) der Universität Stuttgart	FRG
NKS-4	"	"
PTSE-2	Oak Ridge National Laboratory	USA
Spinning Cylinder I	Atomic Energy Authority (AEA) Risley, United Kingdom	UK
Spinning Cylinder II	"	"
Step B PTS	Japan Power and Engineering Inspection Corporation (JAPEIC)	JAPAN

Table 2. Organizations participating in the Project FALSIRE Workshop, Boston, May 1990.

Organization	Country
Atomic Energy Authority (AEA)	UK
B&W Nuclear Services	USA
Battelle	USA
Central Research Institute of Electric Power Industry (CRIEPI)	Japan
Centre D'Etudes Nuclearies de Saclay	France
Combustion Engineering (CE)	USA
Electricite de France (EDF)	France
National Committee for Nuclear and Alternative Energies (ENEA-DISP)	Italy
Fraunhofer Institut fur Werkstoffmechanik (IWM)	FRG
Gesellschaft fur Reaktorsicherheit (GRS)	FRG
Japan Power and Engineering Inspection Corporation (JAPEIC)	Japan
Mitsubishi Heavy Industries (MHI)	Japan
Novetech	USA
Nuclear Electric	UK
Nuclear Energy Agency-OECD	France
Nuclear Installations Inspectorate	UK
Nuclear Regulatory Commission (NRC)	USA
Oak Ridge National Laboratory (ORNL)	USA
Paul Scherrer Institut	Switzerland
Southwest Research Institute (SWRI)	USA
Materialprüfungsanstalt (MPA) der Universität Stuttgart	FRG
Technical Research Center (VTT)	Finland
University of Maryland	USA
University of Tennessee	USA
University of Tokyo	Japan

The experiments utilized in Project FALSIRE were designed to examine various aspects of crack growth in RPV steels under pressurized-thermal-shock (PTS) loading conditions. These conditions were achieved in three of the experiments by internally pressurizing a heated vessel containing a sharp crack and thermally shocking it with a coolant on the inner (NKS-3 and 4) or outer (PTSE-2) surface. In the series of spinning cylinder experiments, a thick cylinder with a deep crack on the inner surface was thermally shocked with a water spray while simultaneously spinning the cylinder about its axis in a specially-constructed rig. The Japanese Step B test utilized a large surface-cracked plate subjected to combined mechanical loads of tension and bending coordinated with a thermal shock of the cracked surface to model PTS loading conditions. Data from the experiments provided in the CSNI/FAG problem statements included pretest material characterization, geometric parameters, loading histories, instrumentation, and measured results for temperatures, strains, crack-mouth opening displacements (CMODs), and crack-growth histories. A summary of the material toughness, loading conditions, crack geometry and crack growth for each experiment is given in Table 3.

Based on the CSNI/FAG problem statements, twenty-seven participants representing twenty-one organizations performed a total of thirty-nine analyses of the experiments. The analysis techniques employed by the participants included engineering methods (R6, GE/EPRI estimation scheme, DPFAD) and finite-element methods; these techniques were combined with applications of J_R methodology and the French Local Approach. The finite element applications include both two- and three-dimensional models, as well as deformation plasticity and incremental thermo-elastic-plastic constitutive formulations. Crack growth models based on nodal release techniques were utilized to generate the application-mode and generation-mode solutions for several of the experiments. A summary of the analysis methods applied to each experiment is given in Table 4. For each of the experiments, analysis results provided estimates of variables including crack growth, CMOD, temperatures, strains, stresses and applied J and K values. Conditions of crack stability and instability were identified in the experiments. Where possible, computed values were compared with measured data.

Table 3. Summary of Project FALSIRE reference experiments.

Experiment (Place)	Material[a] Toughness	Loading	Crack Geometry	Crack Growth
NKS-3 (MPA, FRG)	A_v^{US} = 95 J, T_{NDT} = 60°C	Thermal shock, axial tension, internal pressure (constant)	Circumferential (a/t - 0.3)	Ductile 3.6 mm (Average)
NKS-4 (MPA, FRG)	A_v^{US} = 65 J, T_{NDT} = 120°C	Thermal shock, axial tension, internal pressure (constant)	Partly circumferential (a/t = 0.15)	Ductile 1.5/3.1 mm (Center)
PTSE 2A/B (ORNL, USA)	A_v^{US} = 60 J T_{NDT} = 75°C	Thermal shock, internal pressure (transient)	Axial (a/t = 0.1/0.29)	Ductile 11.1/3.7 mm Brittle 16.8/32.7 mm Unstable -/68.8 mm
Spin Cyl. I (AEA, UK)	A_v^{US} = 90 J	Rotation of specimen	Axial (a/t = 0.54)	Ductile 2.8 mm (Average)
Spin Cyl. II (AEA, UK)	A_v^{US} = 110 J	Thermal shock	Axial (a/t = 0.52)	Ductile 0 - 0.75 mm
Step B PTS (JAPEIC, JAPAN)	A_v^{US} = 100 J, T_{NDT} = 139°C	Thermal shock, tension, and bending	Surface (a/t = 0.14)	Ductile 0.3 - 1.0 mm

[a] A_v^{US} = Charpy V-notch upper-shelf energy (J)

Table 4. Summary of Project FALSIRE analysis techniques[a].

Analysis No.	NKS-3	NKS-4	PTSE-2	S.C. I/II
1	FE; JR	FE; JR	FE; JR	FE; JR
2	FE; JR, LA	FE; JR	FE: JR	FE; JR
3	FE; JR	FE; JR	FE; JR	A1; FE
4	FE; JR, LA	FE; JR	FE; JR	WF; FE
5	FE; JR	ES; J/T	FE; JR	ES; J/T
6	FE; JR	ES; R6/1	FE; JR	A2
7	FE; JR		ES; J/T	ES; R6/1
8	ES; J/T		ES	
9	ES; R6/1			

[a]FE = Finite Element Method
ES = Estimation Scheme
A1 = Analytic Solution with Numerical Integration
A2 = Handbook Analysis of Statically Indeterminate Model
JR = R-Curve Approach
J/T = J/Tearing Modulus Approach
LA = Local Approach
R6/1 = R6 Method/Option 1
WF =Weight Function Method

Comparisons of a portion of the solution results for five of the experiments* are given in the next section. This is followed by discussion of the results and some observations regarding predictive capabilities of the fracture methodologies used in assessing these experiments.

2 COMPARISON OF PROJECT FALSIRE SOLUTIONS

2.1 NKS-3

The NKS-3 pressurized-thermal-shock experiment (Sauter 1987) was performed with a thick-walled hollow cylinder (thickness 200 mm; inner diameter 400 mm) containing a circumferential flaw on the inner surface having an average depth of ~62.8 mm (see Fig. 1a). The test piece was first loaded with an axial tensile load of 100 MN and by pressurized water (30 MPa, 330°C) in the cylinder volume. Thermal shock cooling of the inner cylinder surface was performed by means of two high pressure pumps, spraying cold water (20°C) towards the inner cylinder surface over the whole test length of the cylinder through evenly distributed nozzles. These loading conditions produced a stress field on the circumferential plane of the test vessel that approximates the stress field on a longitudinal plane of a reactor pressure vessel. Results from measurements of stable crack growth on the fracture surface indicated an average measured crack extension of ~3.6 mm around the circumference of the flaw.

Comparisons of the NKS-3 analysis results are given in Figs. 2–3 for time histories of CMOD (Fig. 2) and the computed J-integral (Fig. 3). The methodology employed in each of the analyses represented in Figs 2–3 can be found in Table 4. Based on small-specimen J_R-curves for the NKS-3 test material (Sievers 1987), the J-integral results in Fig. 3 imply stable crack growth in the range of 2.8 - 4.8 mm, which bounds the average measured values of 3.6 mm.

*The test statement for the Japanese Step B test was not made available to the CSNI/FAG early enough for distribution to the participating analysts prior to the Project FALSIRE workshop. Consequently, for the Step B experiment, only the analysis performed by the testing organization was presented at the workshop; that analysis is not included here.

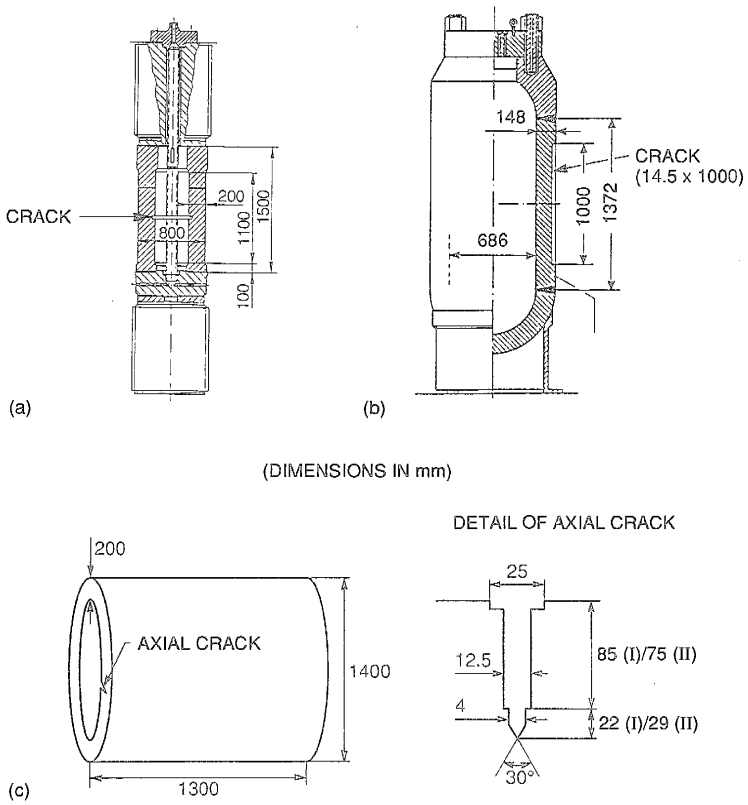

Fig. 1 Geometry of specimens from large-scale PTS experiments analyzed in Project FALSIRE: (a) NKS-3 and 4; (b) PTSE-2; (c) spinning cylinder I and II.

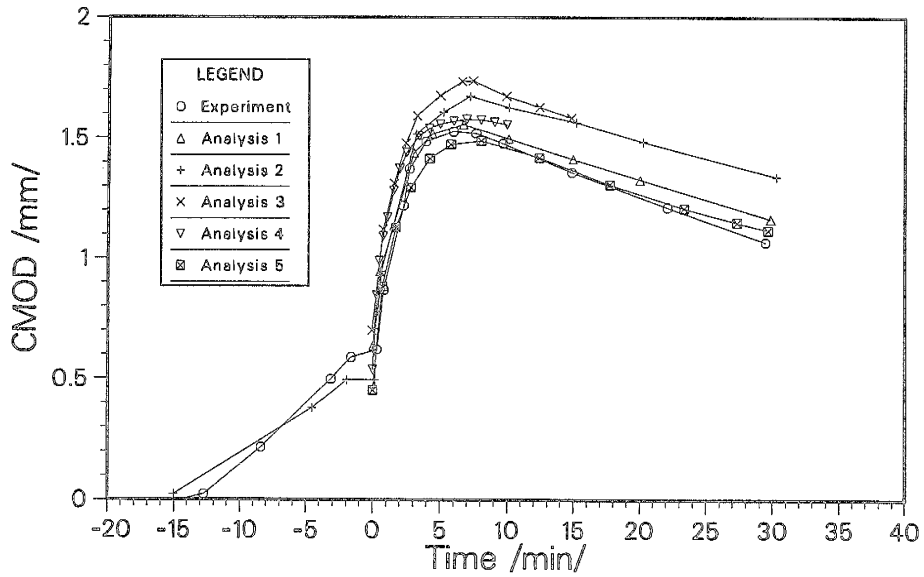

Fig. 2 Comparison of solutions for CMOD versus time for NKS-3 experiment.

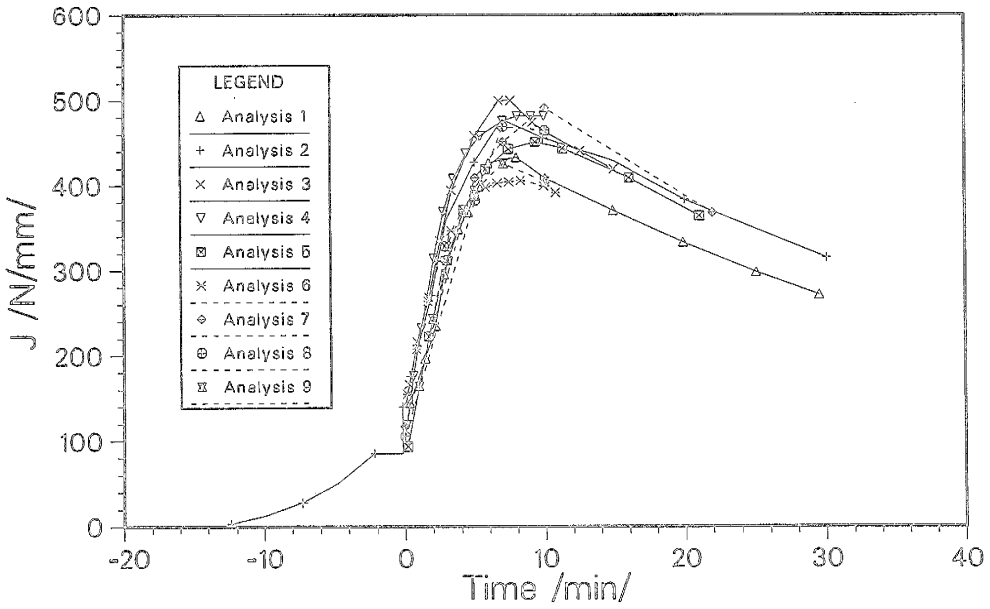

Fig. 3 Comparison of solutions for J-integral versus time for NKS-3 experiment

2.2 NKS-4

The NKS-4 experiment (Sauter et al. 1988) examined crack-growth behavior of two symmetrically opposed semi-elliptical surface cracks in a low-toughness material. Each crack has a ratio of length to depth of 6:1 and a maximum depth of ~30 mm. The cracks were produced by means of spark erosion and fatiguing procedures. The test rig and procedures used to test the NKS-4 specimen were essentially the same as those described in the previous section for NKS-3. The NKS-4 experiment was performed using two thermal-shock transients (identified as NKS-4/A and NKS-4/B), the first of which produced a reduced thermal loading due to mechanical problems with the cooling water flow. The NKS-4/A transient produced a maximum crack growth of ~1.5 mm in the radial direction. The NKS-4/B transient resulted in a maximum radial growth of 3.1 mm.

Analysis results for CMOD vs time from the solutions for the A transient given in Fig. 4 show a variation of ~35% at the time of maximum crack loading (~200 s). The computed results generally over-estimate the measured data, especially in the startup phase of the transient, when control problems occurred with the coolant flow. In Fig. 5, the time histories of the computed J-integral varied about 60% at maximum load, and predicted a maximum crack growth ranging from 1.5 - 5 mm according to J_R-curve methodology.

2.3 PTSE-2

The details of the PTSE-2 test vessel and flaw geometry (Bryan et al. 1987) are given in Fig. 1(b). An HSST intermediate test vessel was prepared with a plug of specially heat-treated test steel welded into the vessel. The 1-m-long sharp flaw was implanted in the outside surface of the plug by cracking a shallow electron-beam weld under the influence of hydrogen charging.

In the experiment, the flawed vessel was enclosed in an outer test vessel (OTV), which was electrically heated to bring the flawed vessel to the desired uniform initial temperature of about 290°C. A thermal transient is initiated by suddenly injecting chilled water or a methanol-water mixture through an annulus between the test vessel and the other vessel. Pressurization of the test vessel is controlled independently by a system capable of pressures up to about 100 MPa.

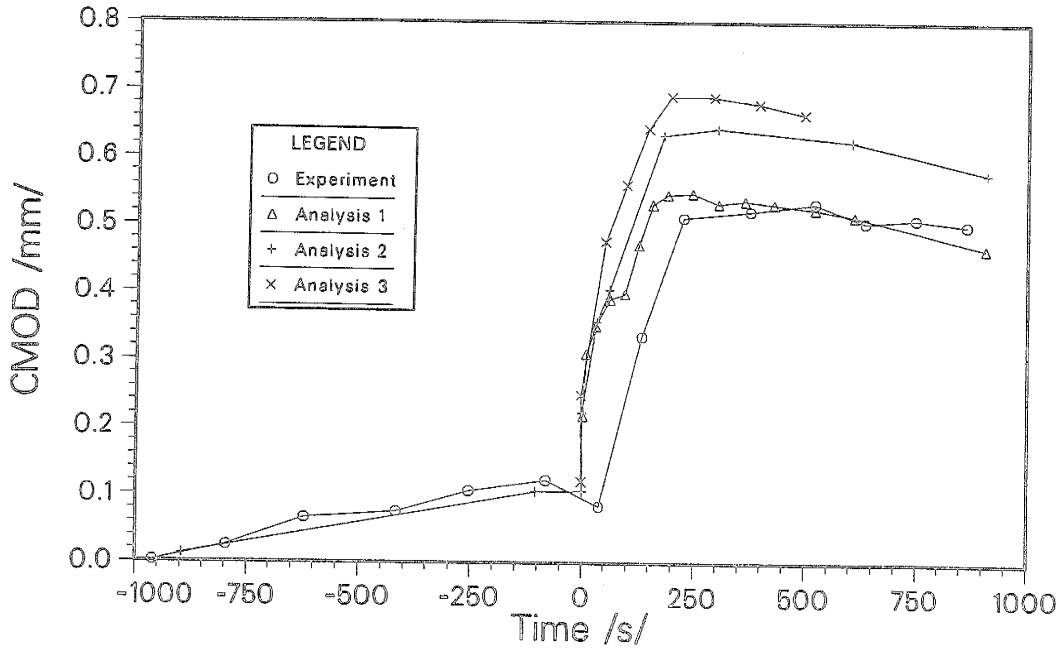

Fig. 4 Comparison of solutions for CMOD versus time for NKS-4 experiment.

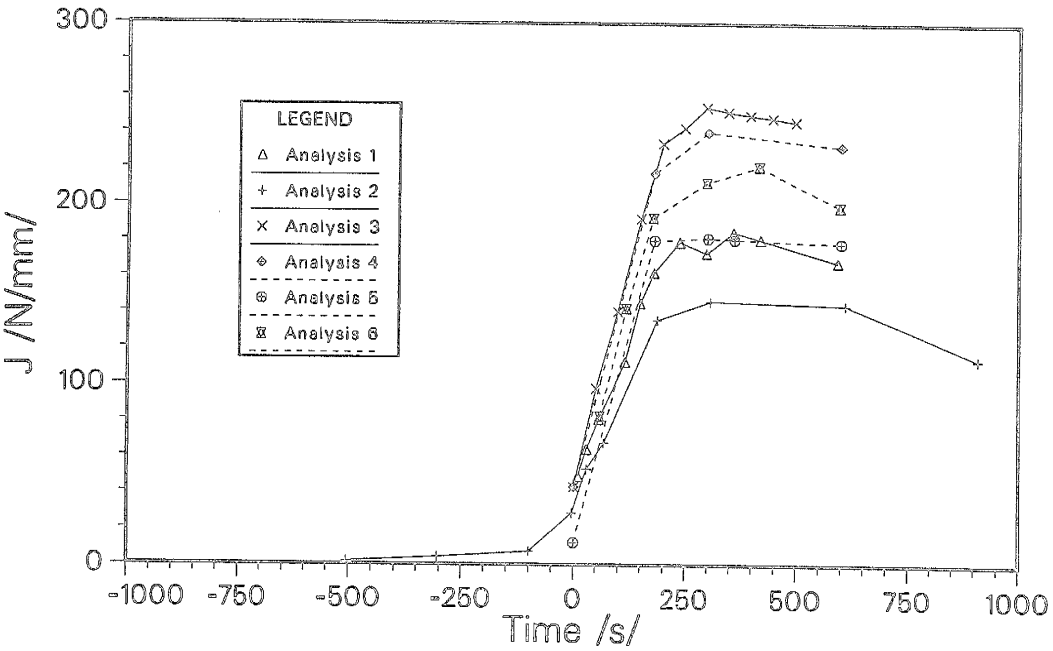

Fig. 5 Comparison of solutions for J-integral versus time for NKS-4 experiment.

The experiment was planned to consist of two transients, of which the first would induce warm prestressing ($\dot{K}_I < 0$) followed by reloading ($\dot{K}_I > 0$) until the crack propagated by cleavage and arrested. The second transient was planned to produce a deep cleavage crack jump with an arrest occurring only after conditions conducive to subsequent unstable tearing were attained. In PTSE-2A, the flaw tore in a ductile mode while K_I was increasing; tearing ceased, presumably when K_I first decreased; tearing resumed at about the time K_I increased again; cleavage crack propagation and arrest occurred; and finally, ductile tearing resumed after crack arrest until pressure was reduced. In PTSE-2B, the extended crack that had developed during the PTSE-2A first tore depthwise and then converted to cleavage. The propagating cleavage fracture arrested and then propagated by ductile tearing until the vessel ruptured.

Finite element analysis results for the PTSE-2A transient are depicted in Fig. 6 in terms of the time history of CMOD at the midplane of the crack. Generally, these results substantially underestimate the measure data, with the difference being as much as 50% for Analysis 5 at the time of the first maximum K_I (~180 s) in the transient. Analysis 5 is performed with posttest material data characterized by a much higher $R_{p0.2}$ and a lower tangent modulus than the pretest data used in the other analyses. Fractographic analyses of the crack surface indicate that measured growth of 5.1 mm occurred during the first phase of the A transient. This crack growth is taken into account in Analysis 2′, but not in Analysis 2. The variations with time of applied J-integral values for the A transient are given in Fig. 7. When the peak J-values from Fig. 7 are compared with small-specimen J_R-curves determined from pretest characterization material in the appropriate temperature range, the initial phase of stable ductile crack growth is estimated to vary from ~1 to 3 mm. This represents a non-conservative estimate when compared with measured data (5.1 mm). Possible explanations for this discrepancy include dependencies in the material data (eg. temperature) and in the fracture toughness (eg. temperature and constraint) that are not taken into account in the analyses.

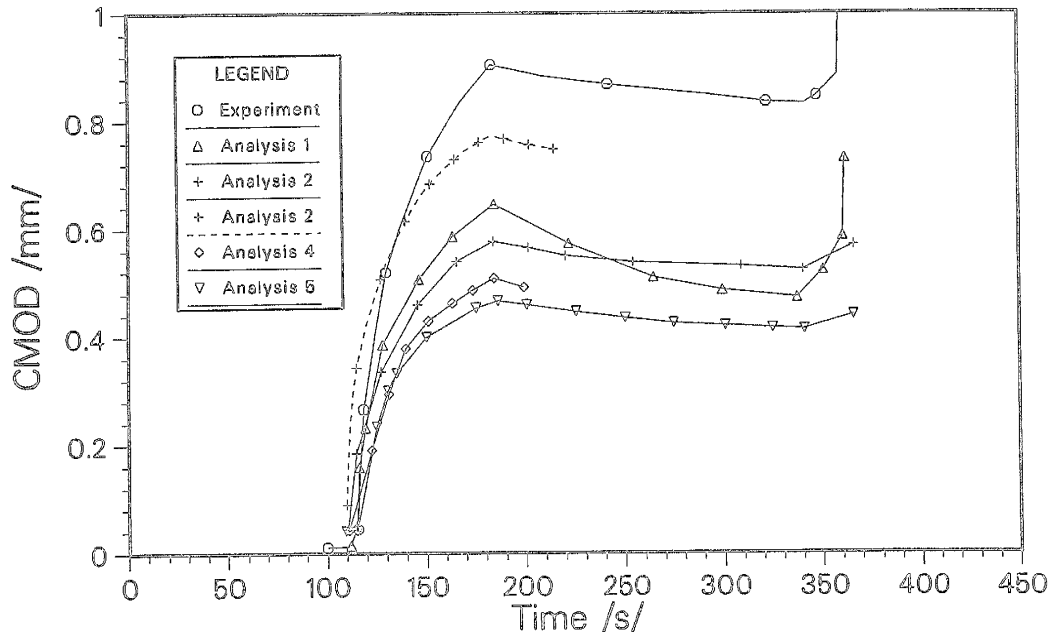

Fig. 6 Comparison of solutions for CMOD versus time for PTSE-2A experiment.

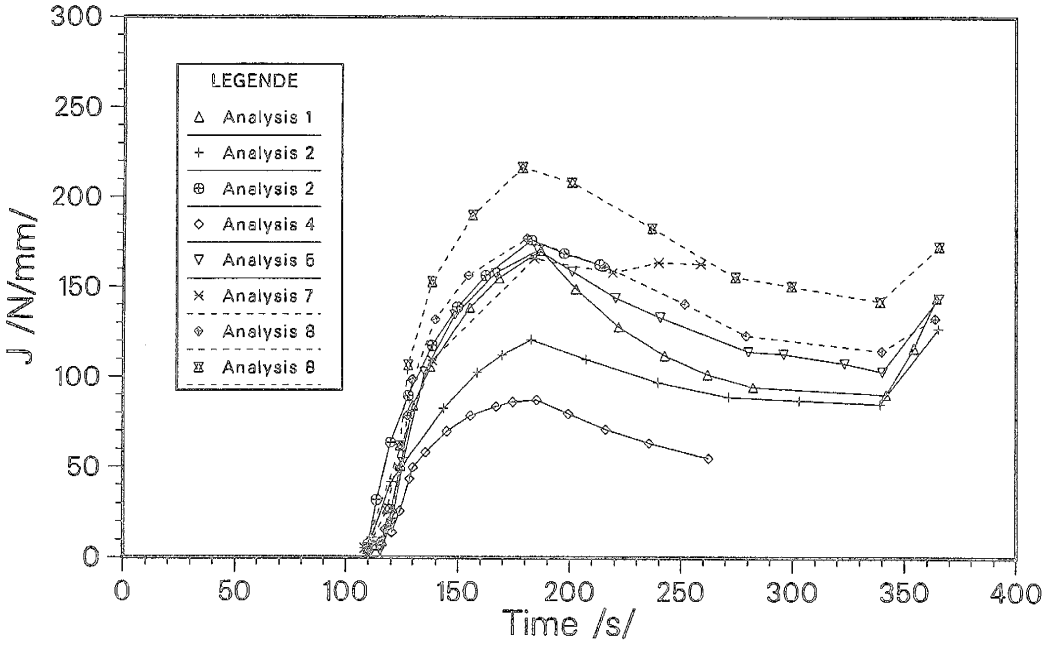

Fig. 7 Comparison of solutions for J-integral versus time for PTSE-2A experiment.

2.4 Spinning Cylinder I

The general arrangement of the spinning cylinder apparatus (Clayton et al. 1985; Lacey et al. 1989) includes an 8-ton cylindrical test specimen (1.3 m long, 1.4 m OD, 200 mm wall thickness as shown in Fig. 1c), which is suspended by a flexible shaft from a single pivoted bearing so that it is free to rotate about the vertical axis. The driving power is provided by a 375 Kw DC motor which is capable of generating a maximum design speed of 3500 rpm at the rotor. Eight 3-Kw heaters mounted vertically within the cylinder enclosure provided the necessary heating to raise the specimen to the required test temperature of 290°C. A stationary water spray system within the cylinder provides the mechanism for thermally shocking the rotating inner surface.

The primary objective of the first test was to provide experimental data which would permit the construction of a J resistance curve. The first test involved the rotation of the cylinder containing a full length axial defect to a speed of 2600 RPM at 290°C. The crack length was measured by the alternating current potential drop method, which indicated ~2.75 mm of stable tearing was generated within contained yielding.

Analysis results for the spinning cylinder I experiment are compared in Fig. 8 for the applied J-integral versus angular velocity for the cylinder. The curve labeled "experimental" in Fig. 8 was generated from the measured crack resistance data (J_R)and the corresponding angular velocity. The J_R-curves reported by Lacey et al. 1989 indicate that the apparent fracture toughness of the cylinder is substantially greater (by ~50%) than that measured from 35 mm CT specimens. Consequently, predictions of crack growth based on the small-specimen J_R-curves substantially overestimate the measured values.

2.5 Spinning Cylinder II

The second spinning cylinder experiment is an investigation of stable crack growth in contained yield for a thick section low alloy steel structure subjected to a severe thermal shock. In the test, ductile crack growth was generated by thermally shocking the inner surface of the cylinder

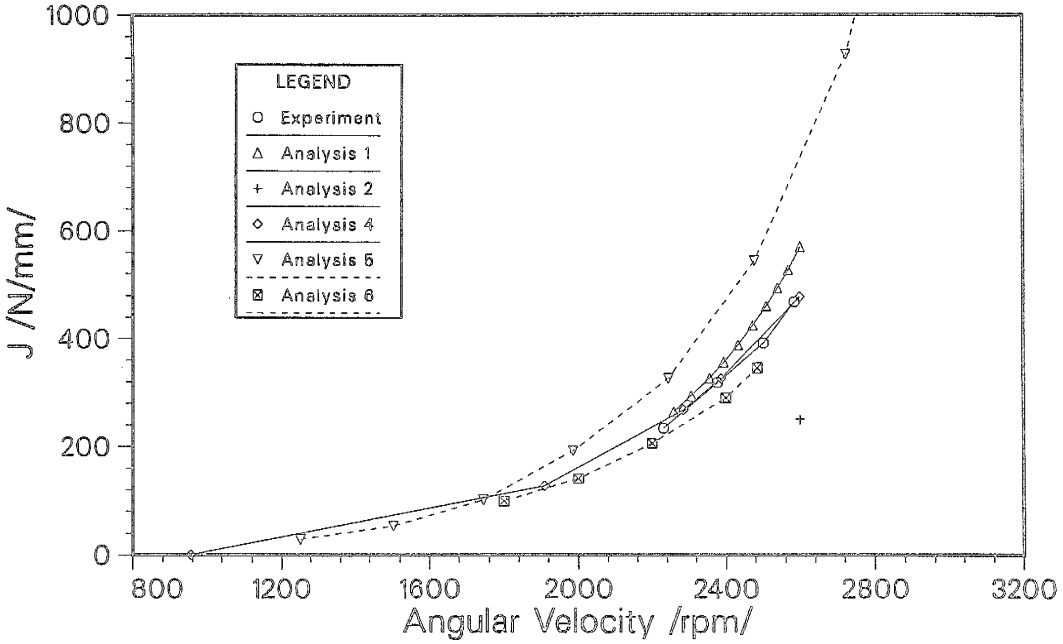

Fig. 8 Comparison of solutions for J-integral versus angular velocity for spinning cylinder I experiment.

containing an axial full-length crack, with a minimal rotational speed. Measured crack growth was a function of axial position, with the maximum of ~0.75 mm occurring at the cylinder midplane.

Analysis results computed for the J-integral versus time from the transient thermal loading are given in Fig. 9. Analysis 1 employed a plane strain finite element formulation and an estimated fracture toughness curve for the cylinder to predict crack growth $\Delta a = 0.26$ mm and peak $J = 310$ N/mm. The analyses based on simplified methods (3, 4, 5, 6, 7) predict crack growth greater or less than the Analysis 1 value depending on the relative magnitude of J as depicted in Fig. 9. Again, the discrepancy between apparent fracture toughness of the cylinder and the small CT specimens was similar to that observed in the first test.

3 DISCUSSION

Although analysis results from the Project FALSIRE Workshop are still being evaluated, several observations can be made concerning predictive capabilities of current fracture assessment methodologies as reflected in the large-scale experiments described in the previous section. Generally, these experiments were designed to verify fracture methodologies under prototypical combinations of geometry, constraint, and loading conditions. However, because complexities of the experiments do not permit a clear separation of the effects of the many variables involved, it has proved difficult to interpret those transients for which expected results were not achieved. Modeling requirements for the experiments incorporate history-dependent mechanical, thermal and body force loadings, temperature-dependent material and fracture toughness properties, residual stress states and three-dimensional effects. Interactions of both cleavage and ductile modes of fracture must be modeled for certain transients. For these reasons, it could be anticipated that comparisons of analysis predictions with available structural data from the experiments would yield results that vary significantly. Examples of these comparisons were

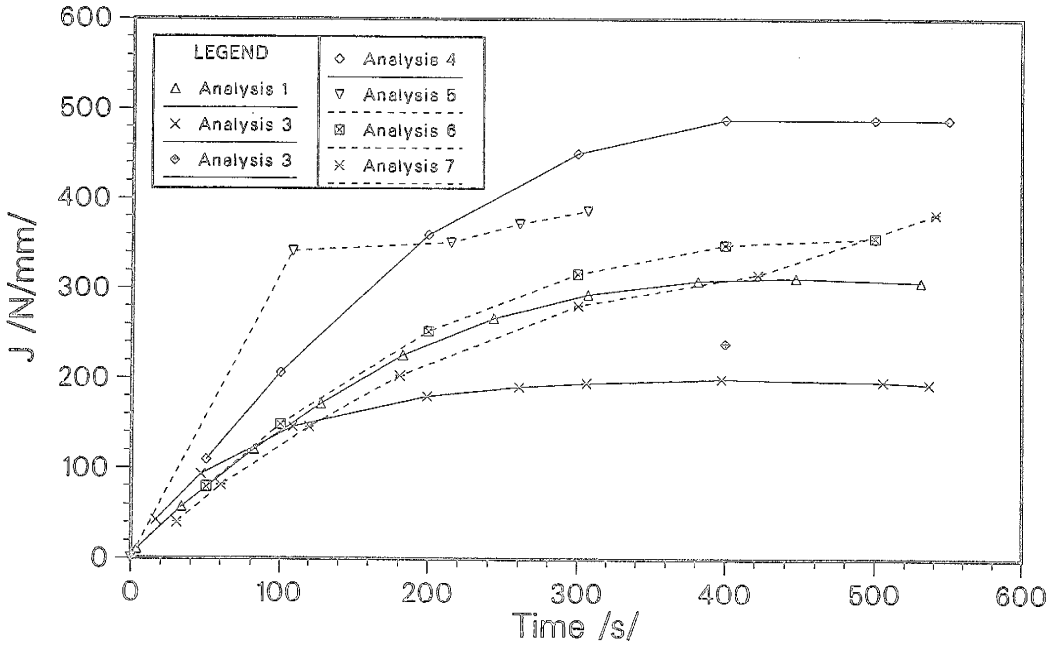

Fig. 9 Comparison of solutions for J-integral versus time for spinning cylinder II experiment.

shown in CMOD vs time plots for experiments NKS-3, -4, and PTSE-2 in Figs. 2, 4, and 6, respectively. The largest differences are seen to occur in the PTSE-2 transient (Fig. 6). All analyses in Fig. 6 assumed material and physical properties to be independent of temperature, which may have contributed to underestimating the measured CMOD in the experiment. These analysis results highlight the importance of obtaining high-quality material properties and structural response data (CMOD, strains, etc.) from the experiments to model structural behavior of the specimen prior to performing fracture mechanics evaluations.

In applications of J_R methodology based on small specimen data, all analyses correctly distinguished between stable crack growth and ductile instability conditions for each experiment. These include both estimation schemes and detailed finite element analyses. However, as a technique to predict crack extension, J_R methodology was partially successful in some cases (NKS experiments), but not in others (PTSE-2, spinning cylinder experiments). In PTSE-2, differences between pretest characterization data and posttest in situ data for material and fracture toughness properties gave rise to questions concerning whether J_R curves from CT specimens were representative of the flawed region of the vessel. None of these temperature-dependent J_R curves were consistent with all phases of ductile tearing observed in PTSE-2. It should be pointed out that the PTSE-2A transient included load-history (i.e. warm-prestressing) effects that were not incorporated into the J_R methodology. The substantial differences between fracture toughness curves generated from the spinning cylinders and from CT specimens focussed attention on other factors. These include the possibility that crack-tip behavior in the spinning cylinder is not characterized by a single correlation parameter. Alternative criteria under consideration include two-parameter models in which K or J is augmented by the next higher-order term T (Al-Ani and Hancock 1991) or Q (O'Dowd and Shih 1991) in the series expansion of the stresses around the crack tip. Other measures considered in dealing with the transfer of small specimen data to large structures include the stress triaxiality parameter q, which is proportional to the ratio of hydrostatic to effective stress (Clausmeyer et al. 1989). Also, the Local Approach has been applied as an alternative to J_R methodology for performing fracture toughness evaluations. For the spinning cylinders, clarification of the initial stress state in front of the crack tip (due to cyclic fatiguing) may be an important consideration.

4 CLOSURE

Preliminary evaluation of the analyses presented at the CSNI/FAG Workshop in Boston showed valuable results. Interpretation of discrepancies revealed in comparisons of these analyses is still ongoing. Additional details concerning comparative analyses of the contributed solutions will be included in the forthcoming final report on Project FALSIRE. Recommendations will be made for future development of fracture methodologies to improve these predictive capabilities. Finally, plans are under way for a second phase of CSNI/FAG fracture assessments that will focus on applications of advanced methods in blind analyses of additional large-scale fracture experiments.

ACKNOWLEDGEMENT

We thank the sponsoring national organizations and the participants (See Table 2) for their cooperation in supplying the experimental data and performing the analytical work for CSNI/FAG Project FALSIRE.

REFERENCES

Al-Ani, A. M. and Hancock, J. M (1991). J-Dominance of Short Cracks in Tension and Bending, Journal of the Mechanics and Physics of Solids, Vol. 39, No. 1, pp. 23–43.

Bryan, R. H., et al. (1987). Pressurized-Thermal Shock Test of 6-in. -Thick Pressure Vessels, PTSE-2: Investigation of Low Tearing Resistance and Warm Prestressing, NUREG/CR-4888 (ORNL-6377), Martin Marietta Energy Systems, Inc., Oak Ridge Nat'l. Lab.

Clausmeyer, H., Kussmaul, K. and Roos, E. (1989). Der Einfluß des Spannungszustandes auf den Versagenseblauf angerissener Bauteile aus Stahl, Mat.-wiss. u. Werkstofftech. 20, pp. 101–117.

Clayton, A. M., et al. (1985). A Spinning Cylinder Tensile Test Facility for Pressure Vessel Steels, 8th SMiRT Conference, Brussels, Belgium, Paper G1/4.

Lacey, D. J.and Leckenby, R. E. (1989). Determination of Upper Shelf Fracture Resistance in the Spinning Cylinder Test Facility, 10th SMiRT Conference, Anaheim, CA., Vol. F, pp. 1–6.

O'Dowd, N. P. and Shih, C. F. (1991). Family of Crack-Tip Fields Characterized by a Triaxiality Parameter: Part I–Structure of Fields, Journal of the Mechanics and Physics of Solids (to be published).

Sauter, A. (1987). Recent Progress in PTS Research at MPA Stuttgart, French-German Seminar, Technical Presentation 1.4.

Sauter, A., Nguyen-Huy, T., Weber, U. and Huber, H. (1988). Behavior of Surface Flaws under Thermal-Mechanical Loading, 14th MPA Seminar, Stuttgart, FRG.

Sievers, J. (1987). Ductile Fracture Mechanical Analyses of Thermal Shock Experiments, 9th SMiRT Conference, Lausanne, Vol. G, pp. 361-368.